

WIMPs during Reheating

Nicolás Bernal^{a, b} and Yong Xu^c

^aNew York University Abu Dhabi

PO Box 129188, Saadiyat Island, Abu Dhabi, United Arab Emirates

^bCentro de Investigaciones, Universidad Antonio Nariño

Carrera 3 este # 47A-15, Bogotá, Colombia

^cBethe Center for Theoretical Physics and Physikalisches Institut, Universität Bonn

Nussallee 12, 53115 Bonn, Germany

E-mail: nicolas.bernal@nyu.edu, yongxu@th.physik.uni-bonn.de

Abstract. Weakly Interacting Massive Particles (WIMPs) are among the best-motivated dark matter candidates. In the standard scenario where the freeze-out occurs well after the end of inflationary reheating, they are in tension with the severe experimental constraints. Here, we investigate the thermal freeze-out of WIMPs occurring *during* reheating, while the inflaton ϕ coherently oscillates in a generic potential $\propto \phi^n$. Depending on the value of n and the spin of the inflaton decaying products, the evolution of the radiation and inflaton energy densities can show distinct features, therefore, having a considerable impact on the freeze-out behavior of WIMPs. As a result of the injection of entropy during reheating, the parameter space compatible with the observed DM relic abundance is enlarged. In particular, the WIMP thermally averaged annihilation cross-section can be several magnitudes lower than that in the standard case. Finally, we discuss the current bounds from dark matter indirect detection experiments, and explore future challenges and opportunities.

Contents

1	Introduction	1
2	Cosmology during Reheating	2
2.1	Fermionic Reheating	4
2.2	Bosonic Reheating	4
3	Dark Matter Production	6
3.1	Freeze out after Reheating	7
3.2	Freeze out during Reheating	7
4	Conclusions	12

1 Introduction

The existence of non-baryonic dark matter (DM) in the Universe is very compelling, as suggested by both astrophysical and cosmological observations [1]. A viable DM candidate has to satisfy several properties: It has to be electromagnetically neutral, stable at the cosmological scales, and non-relativistic at the matter-radiation equality in order to allow structure formation. Finally, it must feature a relic density $\Omega_{\text{dm}} h^2 \simeq 0.12$, accounting for 27% of the total energy budget of the Universe [2, 3].

The most prominent DM production mechanism in the early universe corresponds to the weakly interacting massive particle (WIMP) paradigm [4, 5]. In the standard WIMP scenario, DM has a mass at the electroweak scale and couples to the standard model (SM) thermal plasma with a sizable strength, typical of electroweak interactions. WIMPs reach thermal equilibrium with the SM thermal plasma and eventually *freeze out*, giving rise to the observed DM relic abundance. This DM freeze-out is commonly assumed to occur well after the end of reheating, when the Universe energy density is dominated by SM radiation. To match observations, a thermally averaged annihilation cross-section $\langle\sigma v\rangle = \text{few} \times 10^{-26} \text{ cm}^3/\text{s}$ is typically required [6]. The WIMP mechanism is particularly interesting because it could be tested in a number of complementary ways, including direct, indirect, and collider probes. However, current null experimental results and severe constraints on the natural parameter space motivate some quests beyond the standard WIMP paradigm [4].

There are several possibilities to evade the strong experimental constraints. For example, DM might have feeble interactions with the SM thermal plasma so that it is produced out of equilibrium by the so-called freeze-in mechanism (FIMP) [7–13]. Alternatively, WIMPs might have decoupled during a non-standard cosmological epoch [14], with an annihilation cross section much smaller than the one enforced in the standard case [15]. In general, the production of DM in scenarios with a non-standard expansion phase has recently gained increasing interest; see, e.g., Refs. [15–52]. For earlier work, see also Refs. [53–64]. Moreover, scenarios where freeze-out occurs during reheating are also viable, and in such cases, the freeze-out temperature T_{fo} is higher than the reheating temperature T_{rh} ; note that the latter characterizes the onset of the radiation-dominated era. We note that WIMP scenarios with low reheating temperature have been widely investigated in the literature [28, 60, 65–68], usually triggered by the decay of a long-lived scalar field with an equation-of-state (EoS) parameter $\omega = 0$ and

a constant decay rate Γ_ϕ .¹ Finally, we note that this kind of scenario in which DM reaches chemical equilibrium with the SM bath eliminates the possible overproduction of DM during inflation [83, 84].

In this work, different from the aforementioned literature, we investigate the phenomenology of WIMP freezing out during reheating, where the inflaton field ϕ oscillates around the minimum of a generic potential $\propto \phi^n$. Such potentials naturally arise in a number of inflationary scenarios like the α -attractor T -model [85, 86], or the Starobinsky model [87–90]. In such a case, both the inflaton EoS and its decay rate are modified compared to the usually assumed case (i.e. $n = 2$). In particular, the EoS depends on the shape of the potential $\omega = (n - 2)/(n + 2)$ [91], and Γ_ϕ develops a time dependency [92, 93]. As a consequence, the inflaton and SM energy densities exhibit a non-standard evolution during reheating [94], which has a strong impact on WIMP decoupling.² Depending on the value of n , the inflaton decay products, as well as the reheating temperature, we find that due to the large injection of entropy during reheating, $\langle \sigma v \rangle$ can be several orders of magnitude smaller than in the standard case, thus evading the experimental constraints. We highlight that some regions of the new parameter space are currently being tested by several experiments. Furthermore, we notice that the future CTA experiment might increase our ability to probe different scenarios.

The remainder of the paper is organized as follows. In Sect. 2 we revisit inflationary reheating, in particular, the evolution of the inflaton and the radiation energy densities, with an inflaton oscillating in a potential $\propto \phi^n$. In Sect. 3, we investigate WIMP DM production focusing on the case where freeze-out occurs *during* reheating. Our findings are summarized in Sect. 4.

2 Cosmology during Reheating

We consider an inflaton ϕ that, after the end of inflation, oscillates at the bottom of a monomial potential V of the form

$$V(\phi) = \lambda \frac{\phi^n}{\Lambda^{n-4}}, \quad (2.1)$$

where λ is a dimensionless coupling and Λ an energy scale. Potentials with these types of minima naturally arise in a number of inflationary scenarios, such as the α -attractor T -model [85, 86], or the Starobinsky model [87–90]. The equation of motion for the oscillating inflaton field is given by [91]

$$\ddot{\phi} + (3H + \Gamma_\phi)\dot{\phi} + V'(\phi) = 0, \quad (2.2)$$

where H denotes the Hubble expansion rate and Γ_ϕ the inflaton decay rate. The dots and primes correspond to derivatives with respect to time t and ϕ , respectively. By multiplying the above expression by $\dot{\phi}$, Eq. (2.2) can be rewritten as

$$\frac{d}{dt} \left[\frac{1}{2} \dot{\phi}^2 + V(\phi) \right] = -(3H + \Gamma_\phi) \dot{\phi}^2. \quad (2.3)$$

¹For studies on baryogenesis with a low reheating temperature or during an early matter-dominated phase, see Refs. [65, 69–72] and [73–75], respectively. Furthermore, primordial gravitational wave production in scenarios with an early matter era has recently received particular attention [76–82].

²We note that the phenomenology of FIMPs [92, 93, 95–97] and the QCD axion DM [98] with a time-dependent decay rate has recently been analyzed.

By defining the energy density and pressure of ϕ as $\rho_\phi \equiv \frac{1}{2} \dot{\phi}^2 + V(\phi)$ and $p_\phi \equiv \frac{1}{2} \dot{\phi}^2 - V(\phi)$, together with the equation-of-state parameter $\omega \equiv p_\phi/\rho_\phi = (n-2)/(n+2)$ [91], Eq. (2.3) gives the evolution of ρ_ϕ as

$$\frac{d\rho_\phi}{dt} + \frac{6n}{2+n} H \rho_\phi = -\frac{2n}{2+n} \Gamma_\phi \rho_\phi. \quad (2.4)$$

During reheating, that is, in the range $a_I \ll a \ll a_{\text{rh}}$, where a is the scale factor, and a_I and a_{rh} correspond to the scale factors at the beginning and end of the reheating, respectively, Eq. (2.4) admits the analytical solution

$$\rho_\phi(a) \simeq \rho_\phi(a_{\text{rh}}) \left(\frac{a_{\text{rh}}}{a} \right)^{\frac{6n}{2+n}}. \quad (2.5)$$

As during reheating the Hubble expansion rate is dominated by the inflaton energy density, it follows that

$$H(a) \simeq \begin{cases} H_{\text{rh}} \left(\frac{a_{\text{rh}}}{a} \right)^{\frac{3n}{n+2}} & \text{for } a \leq a_{\text{rh}}, \\ H_{\text{rh}} \left(\frac{a_{\text{rh}}}{a} \right)^2 & \text{for } a_{\text{rh}} \leq a. \end{cases} \quad (2.6)$$

At the end of reheating (i.e., at $a = a_{\text{rh}}$), the inflaton and radiation energy densities are equal, $\rho_R(a_{\text{rh}}) = \rho_\phi(a_{\text{rh}}) = 3 M_P^2 H_{\text{rh}}^2$. Note that in order not to spoil BBN, the reheating temperature must satisfy $T_{\text{rh}} \geq T_{\text{BBN}} \simeq 4$ MeV [99–103].

During reheating, the inflaton transfers its energy density to SM radiation, the end of reheating corresponding to the onset of the SM radiation-dominated era. The SM radiation energy density ρ_R is governed by the Boltzmann equation [93]

$$\frac{d\rho_R}{dt} + 4H \rho_R = +\frac{2n}{2+n} \Gamma_\phi \rho_\phi. \quad (2.7)$$

Using Eq. (2.5), one can solve Eq. (2.7) and further obtain the solution for the evolution of the radiation energy density during reheating

$$\rho_R(a) \simeq \frac{2\sqrt{3}n}{2+n} \frac{M_P}{a^4} \int_{a_I}^a \Gamma_\phi(a') \sqrt{\rho_\phi(a')} a'^3 da', \quad (2.8)$$

where a general scale factor dependence of Γ_ϕ has been assumed. Such a dependence can come, for example, from the inflaton mass parameter. The effective mass m_ϕ for the inflaton field, understood as the second derivative of its potential, is given by

$$m_\phi^2 \equiv \frac{d^2V}{d\phi^2} = n(n-1) \lambda \frac{\phi^{n-2}}{\Lambda^{n-4}} \simeq n(n-1) \lambda \frac{2}{n} \Lambda^{\frac{2(4-n)}{n}} \rho_\phi(a)^{\frac{n-2}{n}}. \quad (2.9)$$

It is interesting to note that for $n \neq 2$, m_ϕ features a field dependence that, in turn, would lead to an inflaton decay rate with a scale factor (or time) dependence.

In the following, two different reheating scenarios will be investigated in which the inflaton either decays to a pair of fermions or bosons via a trilinear coupling.

2.1 Fermionic Reheating

In the case where the inflaton only decays into a pair of fermions Ψ and $\bar{\Psi}$ via a trilinear interaction $y \phi \bar{\Psi} \Psi$, with y being the corresponding Yukawa coupling, the decay rate is given by

$$\Gamma_\phi = \frac{y_{\text{eff}}^2}{8\pi} m_\phi, \quad (2.10)$$

where the effective coupling $y_{\text{eff}} \neq y$ (for $n \neq 2$) is obtained after averaging over oscillations [93, 104, 105]. We will return to our treatment for effective coupling shortly. The evolution of the SM energy density in Eq. (2.8) becomes

$$\rho_R(a) \simeq \frac{\sqrt{3}}{8\pi} \frac{n\sqrt{n(n-1)}}{7-n} \frac{y_{\text{eff}}^2 \lambda^{\frac{1}{n}} M_P \rho_\phi(a_{\text{rh}})^{\frac{n-1}{n}}}{\Lambda^{\frac{n-4}{n}}} \left(\frac{a_{\text{rh}}}{a}\right)^{\frac{6(n-1)}{2+n}} \left[1 - \left(\frac{a_I}{a}\right)^{\frac{2(7-n)}{2+n}}\right], \quad (2.11)$$

and, therefore, the temperature of the SM bath evolves as

$$T(a) \simeq T_{\text{rh}} \times \begin{cases} \left(\frac{a_{\text{rh}}}{a}\right)^{\frac{3}{2} \frac{n-1}{n+2}} & \text{for } n < 7, \\ \frac{a_{\text{rh}}}{a} & \text{for } n > 7. \end{cases} \quad (2.12)$$

The Hubble expansion rate (cf. Eq. (2.6)) can be rewritten as a function of T as

$$H(T) \simeq H_{\text{rh}} \begin{cases} \left(\frac{T}{T_{\text{rh}}}\right)^{\frac{2n}{n-1}} & \text{for } n < 7, \\ \left(\frac{T}{T_{\text{rh}}}\right)^{\frac{3n}{n+2}} & \text{for } n > 7. \end{cases} \quad (2.13)$$

Before closing this subsection, we note that for the case with $n = 2$ where the inflaton oscillates in a quadratic potential with an EoS parameter $\omega = 0$, the standard dependences with the scale factor $\rho_R(a) \propto a^{-3/2}$ and $T(a) \propto a^{-3/8}$ are reproduced.

2.2 Bosonic Reheating

Alternatively, if the inflaton only decays into a pair of bosons S through the interaction $\mu \phi S S$, with μ being a coupling with mass dimension, the decay rate is instead

$$\Gamma_\phi = \frac{\mu_{\text{eff}}^2}{8\pi m_\phi}, \quad (2.14)$$

where again the effective coupling $\mu_{\text{eff}} \neq \mu$ (if $n \neq 2$) can be obtained after averaging over oscillations. Using a procedure similar to the previous fermionic case, one sees that the SM energy density scales as

$$\rho_R(a) \simeq \frac{\sqrt{3}}{8\pi} \frac{1}{1+2n} \sqrt{\frac{n}{n-1}} \frac{\mu_{\text{eff}}^2}{\lambda^{1/n}} M_P \Lambda^{\frac{n-4}{n}} \rho_\phi(a_{\text{rh}})^{\frac{1}{n}} \left(\frac{a_{\text{rh}}}{a}\right)^{\frac{6}{2+n}} \left[1 - \left(\frac{a_I}{a}\right)^{\frac{2(1+2n)}{2+n}}\right], \quad (2.15)$$

with which the SM temperature evolves as

$$T(a) \simeq T_{\text{rh}} \left(\frac{a_{\text{rh}}}{a}\right)^{\frac{3}{2} \frac{1}{2+n}}, \quad (2.16)$$

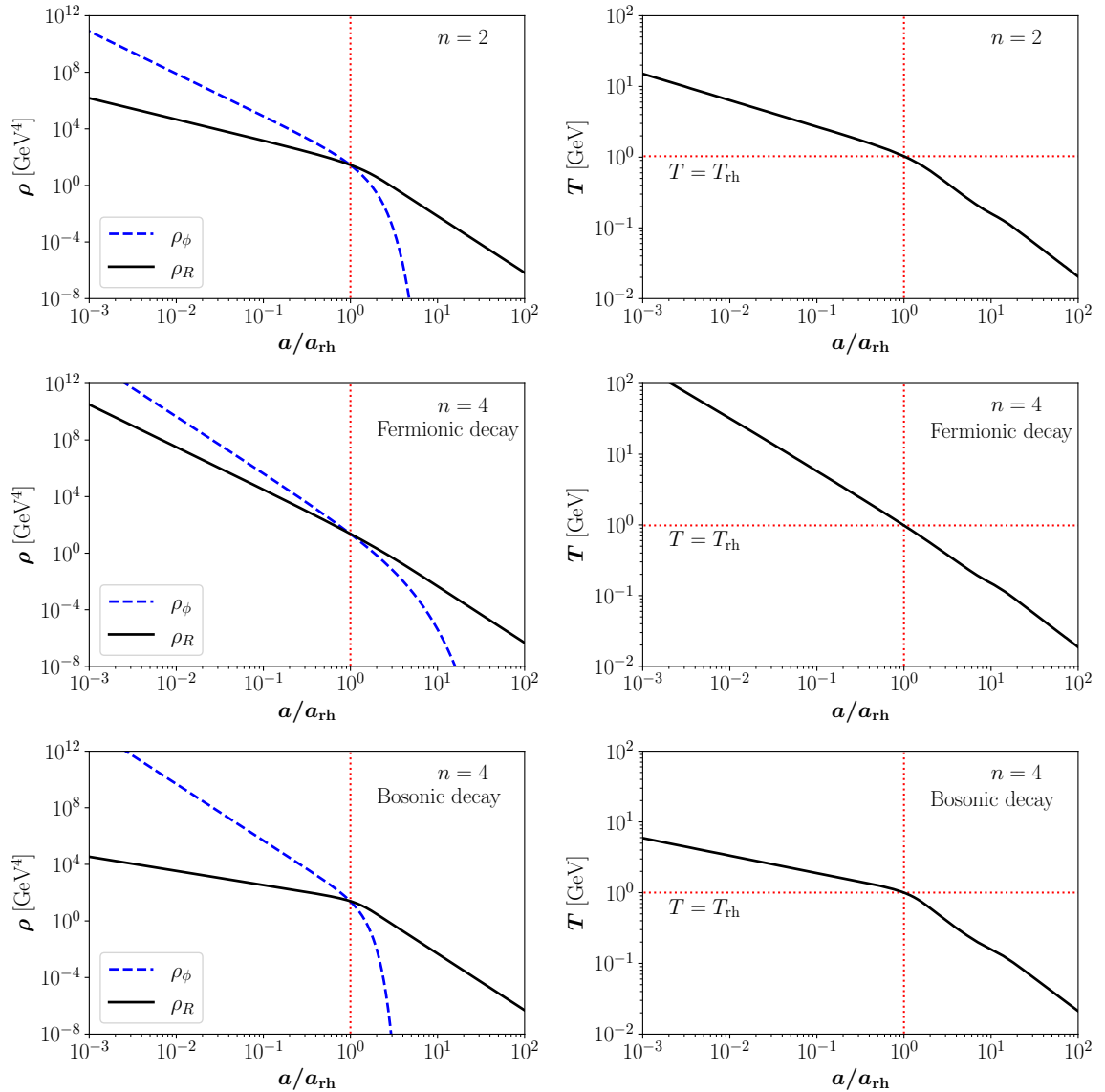


Figure 1. Left: Numerical evolution of the energy densities of the SM (solid black) and ϕ (dashed blue), as a function of the scale factor, for $T_{\text{rh}} = 1$ GeV. Right: Corresponding evolution of the SM temperature.

and Hubble as

$$H(T) \simeq H_{\text{rh}} \left(\frac{T}{T_{\text{rh}}} \right)^{2n}, \quad (2.17)$$

during reheating.

In Fig. 1, the left panels depict the evolution of both the SM radiation (solid black) and the inflaton (dashed blue) energy densities, as a function of the scale factor, for $T_{\text{rh}} = 1$ GeV. The corresponding evolution of the SM bath temperature is shown in the right panels. We note that the bump at $T \sim 0.1$ GeV is due to the QCD phase transition, where the latter leads to a sudden decrease of effective relativistic degrees of freedom in the thermal plasma. The upper panels correspond to the case $n = 2$, where the effects of bosonic and fermionic

decays are equivalent. During reheating, $\rho_\phi \propto a^{-3}$, $\rho_R \propto a^{-3/2}$, and $T \propto a^{-3/8}$. The middle and lower panels correspond to $n = 4$ with fermionic or bosonic decay, respectively. For the first case, $\rho_R \propto a^{-3}$ (and $T \propto a^{-3/4}$) while for the latter case, $\rho_R \propto a^{-1}$ (and $T \propto a^{-1/4}$). Note that to numerically solve the Boltzmann equations for ρ_ϕ and ρ_R , the values of the effective couplings appearing in the decay rates are needed, which shall be obtained numerically [93]. Instead, here we fix T_{rh} and then calculate the effective coupling values so that the reheating temperature matches the desired value. Let us remind the reader that the reheating temperature has been defined as $\rho_R(T_{\text{rh}}) = \rho_\phi(T_{\text{rh}}) = 3 M_P^2 H_{\text{rh}}^2$.

Before proceeding, a comment on the preheating effect is necessary. With the help of lattice simulations, it has been shown that, during reheating, the EoS parameter $\omega \rightarrow 1/3$ for $n \gtrsim 3$ due to inflaton fragmentation and parametric resonance [106–109]. This implies that preheating efficiently drives the Universe to a radiation-dominated phase. However, to fully deplete the inflaton energy, perturbative decay through trilinear couplings between the inflaton and the daughter particles is still required, which is expected to occur in the last stage of the heating process after inflation [107]. Note that for efficient inflaton energy transfer via preheating, sizable couplings are usually required, which could spoil the inflaton potential and inflationary predictions due to loop corrections. Furthermore, in the literature, coherent oscillations of the inflaton condensate have been found to break down [110], which could delay preheating. It has also been shown that depending on the spin of the daughter particles, preheating might be shut down due to the large effective vacuum expectation value of the Higgs field [111]. In this work, we are interested in low-reheating-temperature scenarios, so we assume small inflaton couplings to daughter particles, in which case preheating effects are not expected to be efficient. Thereafter, throughout this work, we will focus on the perturbative reheating scenario.

Having understood possible cosmological histories for the background, in the next section the evolution of the DM number density will be studied, taking particular care to the case where DM freezes out during reheating.

3 Dark Matter Production

The evolution of the DM number density n_{dm} is governed by the Boltzmann equation

$$\frac{dn_{\text{dm}}}{dt} + 3 H n_{\text{dm}} = -\langle\sigma v\rangle (n_{\text{dm}}^2 - n_{\text{eq}}^2), \quad (3.1)$$

with the Hubble expansion rate

$$H^2 = \frac{\rho_R + \rho_\phi}{3 M_P^2}. \quad (3.2)$$

$n_{\text{eq}}(T)$ corresponds to the equilibrium number density given by

$$n_{\text{eq}}(T) \simeq g \left(\frac{m T}{2\pi} \right)^{3/2} e^{-\frac{m}{T}} \quad (3.3)$$

for non-relativistic particles, where m and g denote the mass and the number of degrees of freedom of the DM field, respectively. In this work, we focus on a temperature-independent cross section, which corresponds to an S -wave dominated interaction. We note that direct production of DM out of the inflaton decay may also be relevant. In that case, Eq. (3.1) would have an additional term $\propto 2 \text{Br} \Gamma_\phi n_\phi$, where Br denotes the branching ratio of the

inflaton decay into a couple of DM particles, and n_ϕ is the inflaton number density. Here we focus on the effect of the time dependence of Γ_ϕ on the evolution of the WIMP thermal production, and therefore, in the following analysis this contribution will be omitted.³ Finally, for a discussion regarding DM production during the SM thermalization process, we refer the reader to Refs. [112–116].

3.1 Freeze out after Reheating

We first revisit the standard scenario, where DM freeze-out occurs well *after* reheating, in the standard radiation-dominated era. In this case, since the SM entropy is conserved during and after the DM freeze-out, Eq. (3.1) can conveniently be rewritten as

$$\frac{dY}{dx} = -\frac{\langle\sigma v\rangle s}{Hx} (Y^2 - Y_{\text{eq}}^2), \quad (3.4)$$

where $x \equiv m/T$, the DM yield $Y \equiv n_{\text{dm}}/s$, and the SM entropy density $s(T) = \frac{2\pi^2}{45} g_{\star s} T^3$, with $g_{\star s}(T)$ the number of relativistic degrees of freedom that contribute to the SM entropy. Taking into account that in a radiation-dominated era $H(T) = \sqrt{\frac{\rho_R}{3M_P^2}} = \frac{\pi}{3} \sqrt{\frac{g_\star(T)}{10}} \frac{T^2}{M_P}$, with $g_\star(T)$ being the number of relativistic degrees of freedom contributing to the SM energy density, Eq. (3.4) admits the standard approximate solution

$$Y_0 \simeq \frac{15}{2\pi g_{\star s}} \sqrt{\frac{g_\star}{10}} \frac{1}{M_P T_{\text{fo}} \langle\sigma v\rangle}, \quad (3.5)$$

where Y_0 corresponds to the DM yield at present, long after freeze-out. To match the whole observed DM relic density, it is required that

$$m Y_0 = \Omega_{\text{dm}} h^2 \frac{1}{s_0} \frac{\rho_c}{h^2} \simeq 4.3 \times 10^{-10} \text{ GeV}, \quad (3.6)$$

with $\rho_c \simeq 1.05 \times 10^{-5} h^2 \text{ GeV/cm}^3$ being the critical energy density, $s_0 \simeq 2.69 \times 10^3 \text{ cm}^{-3}$ the present entropy density [117], and $\Omega_{\text{dm}} h^2 \simeq 0.12$ the observed DM relic abundance [2].

The temperature T_{fo} at which the DM freeze-out occurs, or equivalently $x_{\text{fo}} \equiv \frac{m}{T_{\text{fo}}}$, is defined by the equality $\left. \frac{n_{\text{eq}} \langle\sigma v\rangle}{H} \right|_{x_{\text{fo}}} = 1$, and given by

$$x_{\text{fo}} = -\frac{1}{2} \mathcal{W}_{-1} \left[-\frac{8\pi^5 g_\star}{45 g^2} \frac{1}{(M_P m \langle\sigma v\rangle)^2} \right], \quad (3.7)$$

where \mathcal{W}_{-1} is the -1 branch of the Lambert function. The observed DM relic abundance is typically matched for cross-sections at the electroweak scale $\langle\sigma v\rangle = \mathcal{O}(10^{-9}) \text{ GeV}^{-2}$ which corresponds to $\mathcal{O}(10^{-26}) \text{ cm}^3/\text{s}$ and $x_{\text{fo}} \sim 25$, with a small logarithmic dependence on the DM mass [6].

3.2 Freeze out during Reheating

Even if the DM freeze-out is typically assumed to occur well *after* the end of reheating, when the Universe is radiation dominated, this is not guaranteed. Alternatively, DM freeze-out could occur *during* reheating. In this case, the SM entropy is not conserved because of the

³This is typically a good assumption as long as $\text{Br} \lesssim 10^{-4} m/(100 \text{ GeV})$ [15, 28].

decay of the inflaton into SM particles. Therefore, instead of Eq. (3.4), it is more convenient to rewrite Eq. (3.1) as

$$\frac{dN}{da} = -\frac{\langle\sigma v\rangle}{H a^4} (N^2 - N_{\text{eq}}^2), \quad (3.8)$$

where $N \equiv a^3 n_{\text{dm}}$ and $N_{\text{eq}} \equiv a^3 n_{\text{eq}}$. Using Eq. (2.6) for the Hubble parameter during reheating, Eq. (3.8) can be analytically solved as

$$N(a_{\text{rh}}) \simeq \frac{6}{2+n} \frac{H_{\text{rh}}}{\langle\sigma v\rangle} a_{\text{rh}}^3 \left(\frac{a_{\text{rh}}}{a_{\text{fo}}}\right)^{\frac{-6}{2+n}}, \quad (3.9)$$

where a_{fo} and a_{rh} correspond to the scale factor when $T = T_{\text{fo}}$ and $T = T_{\text{rh}}$, respectively. After reheating, namely, for $a > a_{\text{rh}}$, the SM entropy is conserved, and therefore $Y_0 \simeq Y(a_{\text{rh}})$, implying

$$Y_0 = \frac{N(a_{\text{rh}})}{s(a_{\text{rh}}) a_{\text{rh}}^3} \simeq \frac{6}{2+n} \frac{45}{2\pi^2 g_{*s}} \frac{H_{\text{rh}}}{\langle\sigma v\rangle T_{\text{rh}}^3} \times \begin{cases} \left(\frac{T_{\text{rh}}}{T_{\text{fo}}}\right)^{\frac{4}{n-1}} & \text{for fermionic decay,} \\ \left(\frac{T_{\text{rh}}}{T_{\text{fo}}}\right)^4 & \text{for bosonic decay,} \end{cases} \quad (3.10)$$

for $n < 7$ in the case of fermionic decay. This assumption will be followed from now on. We note that, in the era after the freeze-out and before the end of reheating, the DM yield evolves as $Y(T) \propto (aT)^{-3}$, which corresponds to

$$Y(T) \propto \begin{cases} T^{\frac{7-n}{n-1}} & \text{for fermionic decay,} \\ T^{1+2n} & \text{for bosonic decay.} \end{cases} \quad (3.11)$$

Examples of the evolution of DM abundance are shown in Fig. 2, for reference points that fit the total observed abundance: the upper panel corresponds to $n = 2$, $T_{\text{rh}} = 1$ GeV, $m = 100$ GeV and $\langle\sigma v\rangle = 10^{-11}$ GeV $^{-2}$, the lower left panel corresponds to a fermionic decay with $n = 4$, $T_{\text{rh}} = 0.1$ GeV, $m = 100$ GeV and $\langle\sigma v\rangle = 6 \times 10^{-10}$ GeV $^{-2}$, and the lower right panel corresponds to a bosonic decay with $n = 4$, $T_{\text{rh}} = 1$ GeV, $m = 40$ GeV and $\langle\sigma v\rangle = 5 \times 10^{-11}$ GeV $^{-2}$. The solid black lines depict the evolution of the DM yield Y , while the dashed black lines show the equilibrium yield Y_{eq} . Furthermore, the red dotted vertical lines show $T = T_{\text{fo}}$ and $T = T_{\text{rh}}$, and the gray horizontal bands correspond to the observed DM abundance $\Omega_{\text{dm}} h^2 \simeq 0.12$ [2].

The evolution of the DM yield depicted in Fig. 2 is obtained by numerically solving the Boltzmann equations (2.4), (2.7), (3.1) and the Friedmann equation (3.2). We have checked that the analytical estimate of the asymptotic value of Y_0 shown in Eq. (3.10) agrees well with the numerical result. Furthermore, the evolution of the DM yield for $T_{\text{fo}} \gg T \gg T_{\text{rh}}$ (that is, $Y \propto x^{-5}$ for $n = 2$, and $Y \propto x^{-1}$ or $Y \propto x^{-9}$ for fermionic or bosonic decays, respectively, and $n = 4$) also matches the analytical expressions of Eq. (3.11). It is worth noticing that in the lower right panel, the DM only reaches chemical equilibrium with the SM bath at $x \simeq 3$.

The contours for the reheating temperature required to match the whole measured DM abundance are shown in Fig. 3, in the parameter space $[m, \langle\sigma v\rangle]$, for bosonic and fermionic decays of the inflaton, and different values of n . The thick black lines correspond to the standard case, where DM freezes out in a radiation-dominated era, whereas the thin black lines to $T_{\text{rh}} = T_{\text{BBN}}$, 10^{-1} GeV, 10^0 GeV and 10^1 GeV. Some constraints apply and are

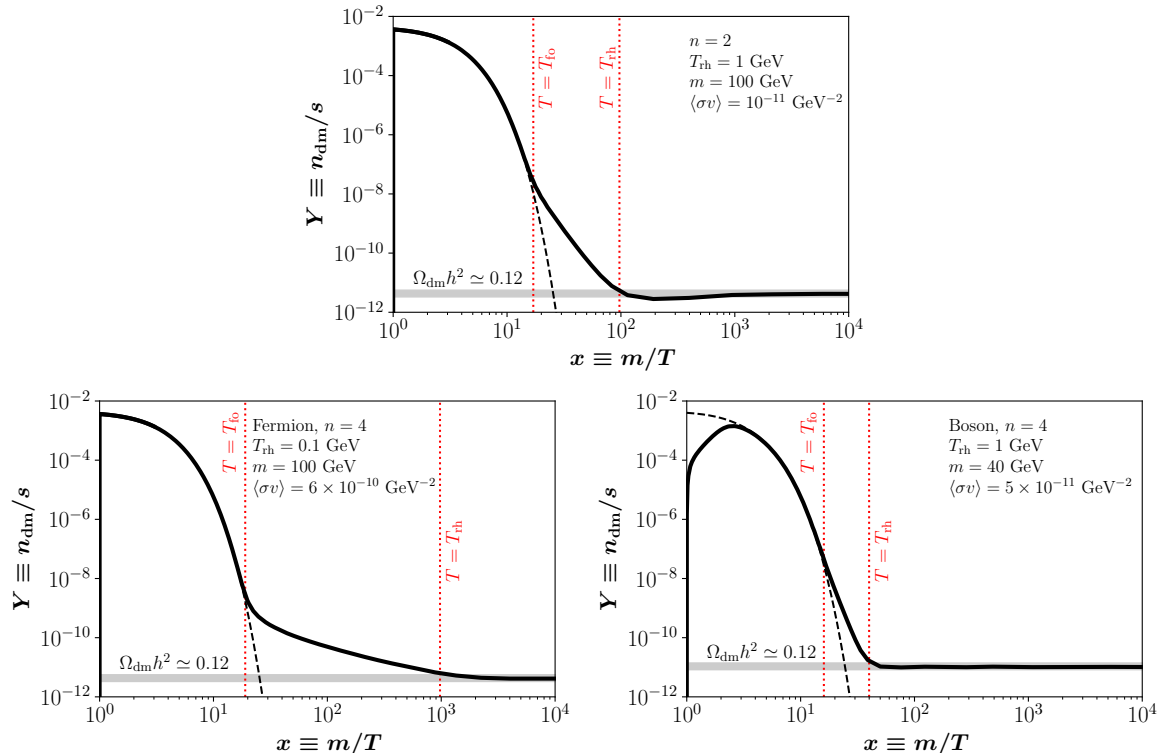


Figure 2. Examples of the evolution of the DM abundance, for different benchmark points described in the text that fit the total observed abundance. The solid black lines show the DM yield Y , whereas the dashed black lines show the equilibrium density. Furthermore, the dotted red vertical lines correspond to $T = T_{\text{fo}}$ and $T = T_{\text{rh}}$, and the gray horizontal bands depict the observed DM abundance $\Omega_{\text{dm}} h^2 \simeq 0.12$.

shown as red regions: *i*) Above the thick black line, corresponding to higher cross sections, DM decouples very late and is therefore underproduced ($\Omega_{\text{dm}} h^2 < 0.12$). *ii*) Reheating temperatures below T_{BBN} are in conflict with cosmological observations, which corresponds to $m \lesssim \mathcal{O}(10^{-1})$ GeV. And *iii*), very small thermally averaged cross sections $\langle\sigma v\rangle$ could not be enough to guarantee chemical equilibrium between the dark and visible sectors. It is worth mentioning that in this case, labeled ‘No freeze-out’, the whole DM relic abundance could be matched, however, the production would not correspond to the WIMP mechanism, but rather to a FIMP scenario, with the usual strong dependence on initial conditions. This case will not be considered in the present analysis.

In Fig. 3, it can be seen that a DM freeze-out during reheating allows exploring smaller cross-sections $\langle\sigma v\rangle$ compared to the usual case where the freeze-out occurs in the standard radiation-dominated case. For example, with $n = 2$ and $T_{\text{rh}} = 10$ GeV, $\langle\sigma v\rangle$ can be as small as $\mathcal{O}(10^{-15})$ GeV $^{-2}$ for a DM mass of ~ 7 TeV. In a scenario with larger T_{rh} , even smaller $\langle\sigma v\rangle$ are allowed for heavier WIMPs. We also note that for a fixed T_{rh} , $\langle\sigma v\rangle$ decreases with increasing m . This is because for heavier WIMPs, freeze-out occurs earlier (i.e., at a larger T_{fo}), which implies a smaller $\langle\sigma v\rangle$. Finally, it should be noted that with increasing n , the parameter space shrinks, as depicted in Fig. 3. The main reason is that the dilution effect becomes less prominent with larger n (that is, the factor $(a_{\text{rh}}/a_{\text{fo}})^{\frac{-6}{2+n}}$ in Eq. (3.9)), and hence a larger $\langle\sigma v\rangle$ is needed to compensate for this. A larger $\langle\sigma v\rangle$ corresponds to a later freeze-out,

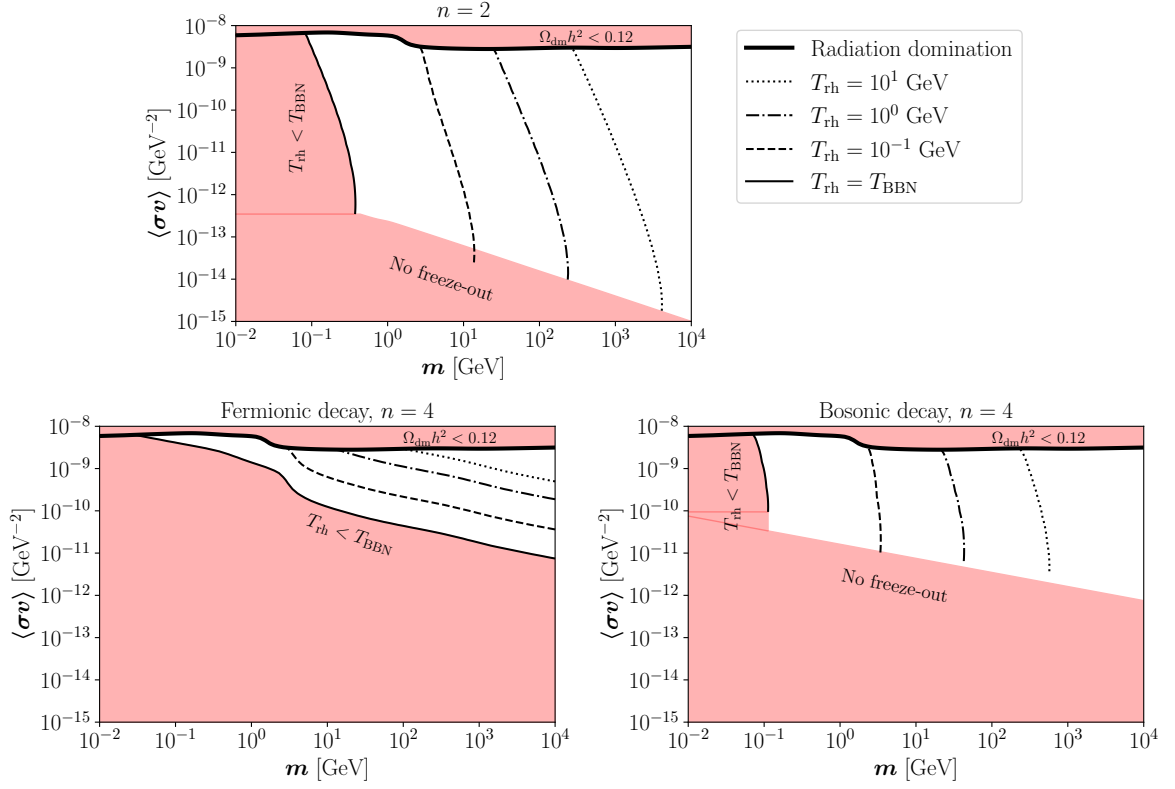


Figure 3. Parameter space that matches the whole observed DM abundance, for $T_{\text{rh}} = T_{\text{BBN}}$ (solid lines), 10^{-1} GeV (dashed), 10^0 GeV (dash-dotted), and 10^1 GeV (dotted). The upper panel corresponds to $n = 2$, while the lower to $n = 4$ and fermionic (left) or bosonic (right) decays of the inflaton. The thick black lines correspond to the standard scenario, where DM freeze-out in the radiation-dominated era. The red areas are disregarded as they generate a DM underabundance ($\Omega_{\text{dm}} < 0.12$), the reheating occurs after BBN ($T_{\text{rh}} < T_{\text{BBN}}$), or DM does not reach chemical equilibrium with the SM (‘No freeze-out’).

where the WIMP densities are smaller, and therefore a smaller dilution is required.

In the present case, DM freezes out during reheating, at a temperature given by

$$x_{\text{fo}} \simeq \begin{cases} \frac{3+n}{2(1-n)} \mathcal{W}_{-1} \left[\frac{2(1-n)}{3+n} \left(\frac{g^2}{(2\pi)^3} \frac{m^2 T_{\text{rh}}^4 \langle \sigma v \rangle^2}{H_{\text{rh}}^2} \right)^{\frac{1-n}{3+n}} \left(\frac{m}{T_{\text{rh}}} \right)^{\frac{4}{3+n}} \right] & \text{for fermions,} \\ \frac{3-4n}{2} \mathcal{W}_{-1} \left[\frac{2}{3-4n} \left(\frac{g^2}{(2\pi)^3} \frac{m^2 T_{\text{rh}}^4 \langle \sigma v \rangle^2}{H_{\text{rh}}^2} \right)^{\frac{1}{3-4n}} \left(\frac{m}{T_{\text{rh}}} \right)^{\frac{4(1-n)}{3-4n}} \right] & \text{for bosons.} \end{cases} \quad (3.12)$$

Figure 4 shows the freeze-out temperature required to match the entire observed DM abundance, as a function of the DM mass, for $T_{\text{rh}} = T_{\text{BBN}}$ (solid lines), 10^{-1} GeV (dashed lines), 10^0 GeV (dash-dotted lines) and 10^1 GeV (dotted lines). The upper panel corresponds to $n = 2$, the lower left to a fermionic decay with $n = 4$, and the lower right to a bosonic decay with $n = 4$. The thick black lines represent the standard freeze-out in radiation domination; cf. Eq. (3.7). Additionally, the lower red bands depict a relativistic freeze-out, i.e. $x_{\text{fo}} \leq 3$. Note that for $n = 2$, the freeze-out temperature can be as low as $x_{\text{fo}} \sim 6$ due to the entropy

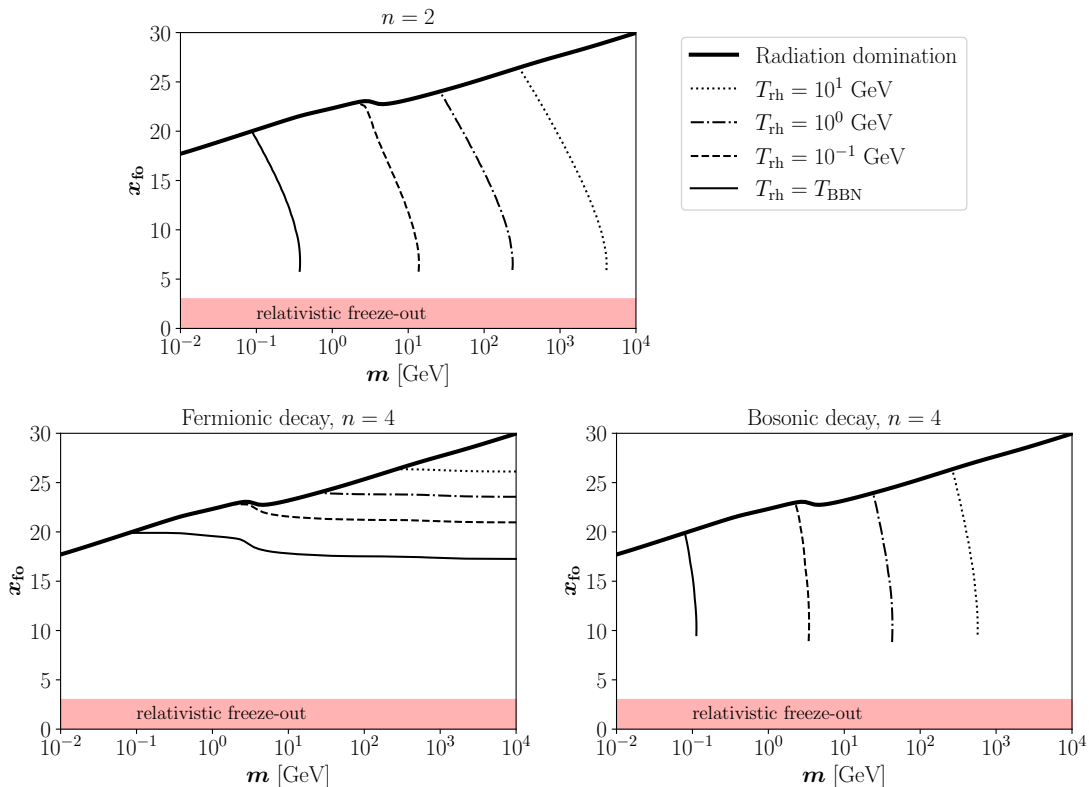


Figure 4. Freeze-out temperature required to match the whole observed DM abundance, as a function of the DM mass, for $T_{\text{rh}} = T_{\text{BBN}}$ (solid lines), 10^{-1} GeV (dashed lines), 10^0 GeV (dotted lines in dashes) and 10^1 GeV (dotted lines). The upper panel corresponds to $n = 2$, while the lower left to a fermionic decay with $n = 4$, and the lower right to a bosonic decay with $n = 4$. The thick black lines represent the standard freeze-out in radiation domination.

dilution effect. For $n = 2$ and $n = 4$ (bosonic), the lines are cut to ensure that WIMPs thermalize; lower values of x_{fo} would correspond to the ‘No freeze-out’ regime depicted in Fig. 3. For a fermionic decay with $n = 4$, x_{fo} tends to be independent of m , with only a small dependence on the relativistic degrees of freedom. Note that the temperature during reheating (for the fermionic case) tends to feature the same scaling as the free radiation for large values of n , cf. Eq. (2.12); this implies that the corresponding freeze-out behavior becomes similar to the standard case. Actually, such a tendency can also be seen in Fig. 4. However, for the bosonic case, due to a different temperature scaling (cf. Eq. (2.16)), the allowed parameter space becomes distinct from the fermionic case with an increase of n . Note that, as argued earlier, in both fermionic and bosonic cases, with increasing n , a larger $\langle\sigma v\rangle$ (corresponding to a later freeze-out with lower T_{fo}) is needed, implying that x_{fo} increases with n , as depicted in Fig. 4.

Before closing this section, we comment on some present and future possibilities of testing the current scenario using the different channels offered by DM indirect detection experiments. In addition to the information given in Fig. 3, Fig. 5 also shows in blue present constraints coming from: *i*) CMB spectral distortions from WIMP annihilation into charged particles [118] (labeled ‘CMB’), *ii*) the combined analysis (labeled ‘combined’) of γ -ray data using Fermi-LAT, HAWC, H.E.S.S., MAGIC, and VERITAS by considering WIMP annihilation to $\tau^+\tau^-$

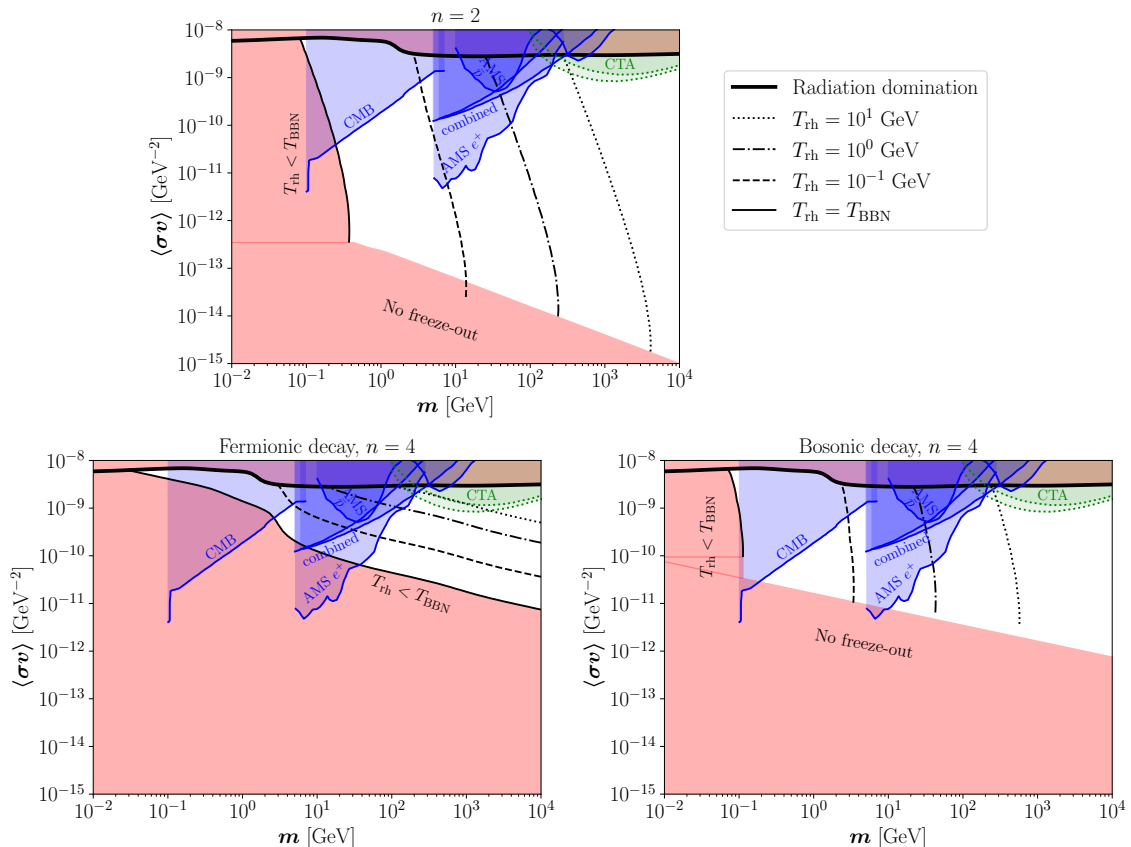


Figure 5. Same as Fig. 3 with current experimental bounds (blue) and future sensitivities (green).

(upper line) and $b\bar{b}$ (lower line) [119], and *iii*) AMS-02 measurements of antimatter in cosmic rays, in the positron [120] and the antiproton [121] channels.⁴ Additionally, Fig. 5 shows in green the projected sensitivity of the ground-based CTA experiment, which could be capable of testing WIMP DM at the TeV scale and above. The upper (lower) green dotted line shows its expected sensitivity for WIMP annihilation to $b\bar{b}$ (W^+W^-) [129]. Note that CTA might be able to probe a large fraction of the TeV-scale WIMPs in the standard scenario, and even a chunk of the parameter space where the freeze-out occurs during reheating, for both fermionic and bosonic decays.

4 Conclusions

Despite the huge experimental efforts over the past decades, the nature of dark matter (DM) remains one of the most challenging and fundamental questions in particle physics. In particular, scenarios where DM is a weakly interacting massive particle (WIMP) reaching thermal equilibrium with the standard model (SM) bath have received immense attention both theoretically and experimentally, but unfortunately no overwhelming evidence for WIMP DM has been found. This motivates a quest beyond the standard WIMP paradigm. An alternative

⁴It is interesting to recall that the bounds presented depends on the DM annihilation channels, and suffer from large uncertainties arising from e.g. assumptions on the DM density profile, the local DM density, and the propagation of charged particles in the interstellar medium [122–128].

is to renounce the thermal nature of DM, as in the FIMP paradigm. However, these kinds of scenario suffer from a strong dependence on the largely unknown initial conditions after cosmological inflation.

In this work, we focus on another avenue where DM remains a thermal relic, but its freeze-out (that is, its departure from chemical equilibrium) occurs *during* (and not after) inflationary reheating. In particular, we investigated a scenario where the inflaton field ϕ coherently oscillates at the bottom of a generic potential $V(\phi) \propto \phi^n$, while decaying into SM particles to reheat the Universe. Depending on the details of the reheating (i.e. the shape of the potential and the coupling between the inflaton and the SM particles), the inflaton and the SM energy density could feature a distinct evolution. Consequently, in this case the behavior of WIMP freeze-out differs from the case where it occurs well after reheating. Due to the dilution effect during reheating, smaller thermally averaged cross-sections $\langle\sigma v\rangle$ becomes compatible with the measured DM relic abundance.

In particular, if DM freezes-out after reheating, one requires $\langle\sigma v\rangle \sim \mathcal{O}(10^{-9}) \text{ GeV}^{-2} \sim \mathcal{O}(10^{-26}) \text{ cm}^3/\text{s}$ to match the observed DM abundance, and a DM freeze-out temperature $x_{\text{fo}} \equiv m/T_{\text{fo}} \sim 25$. Instead, if the freeze-out occurs during reheating while the inflaton oscillates in a quadratic potential ($n = 2$), if $T_{\text{rh}} \sim 1 \text{ GeV}$, $\langle\sigma v\rangle$ could be of the order $\mathcal{O}(10^{-15}) \text{ GeV}^{-2}$ for a WIMP at the TeV scale. Interestingly, a sizable part of the parameter space is in the range of current experiments and future proposals. For instance, for TeV-scale WIMPs, the upcoming CTA could probe the expected cross-sections for DM decoupling after reheating, and a portion of the plane $[m, \langle\sigma v\rangle]$ relevant for the case where DM decouples during reheating.

Acknowledgments

We would like to thank Manuel Drees once again for enlightening discussions. NB received funding from the Patrimonio Aut3nomo - Fondo Nacional de Financiamiento para la Ciencia, la Tecnolog3a y la Innovaci3n Francisco Jos3 de Caldas (MinCiencias - Colombia) grants 80740-465-2020 and 80740-492-2021. NB is also funded by the Spanish FEDER/MCIU-AEI under grant FPA2017-84543-P. This project has received funding/support from the European Union's Horizon 2020 research and innovation program under the Marie Skłodowska-Curie grant agreement No 860881-HIDDeN.

References

- [1] G. Bertone and D. Hooper, *History of dark matter*, *Rev. Mod. Phys.* **90** (2018) 045002 [[1605.04909](#)].
- [2] PLANCK collaboration, *Planck 2018 results. VI. Cosmological parameters*, *Astron. Astrophys.* **641** (2020) A6 [[1807.06209](#)].
- [3] M. Drees, *Dark Matter Theory*, *PoS ICHEP2018* (2019) 730 [[1811.06406](#)].
- [4] G. Arcadi, M. Dutra, P. Ghosh, M. Lindner, Y. Mambrini, M. Pierre et al., *The waning of the WIMP? A review of models, searches, and constraints*, *Eur. Phys. J. C* **78** (2018) 203 [[1703.07364](#)].
- [5] L. Roszkowski, E.M. Sessolo and S. Trojanowski, *WIMP dark matter candidates and searches—current status and future prospects*, *Rept. Prog. Phys.* **81** (2018) 066201 [[1707.06277](#)].

- [6] G. Steigman, B. Dasgupta and J.F. Beacom, *Precise Relic WIMP Abundance and its Impact on Searches for Dark Matter Annihilation*, *Phys. Rev. D* **86** (2012) 023506 [[1204.3622](#)].
- [7] J. McDonald, *Thermally generated gauge singlet scalars as selfinteracting dark matter*, *Phys. Rev. Lett.* **88** (2002) 091304 [[hep-ph/0106249](#)].
- [8] K.-Y. Choi and L. Roszkowski, *E-WIMPs*, *AIP Conf. Proc.* **805** (2005) 30 [[hep-ph/0511003](#)].
- [9] A. Kusenko, *Sterile neutrinos, dark matter, and the pulsar velocities in models with a Higgs singlet*, *Phys. Rev. Lett.* **97** (2006) 241301 [[hep-ph/0609081](#)].
- [10] K. Petraki and A. Kusenko, *Dark-matter sterile neutrinos in models with a gauge singlet in the Higgs sector*, *Phys. Rev. D* **77** (2008) 065014 [[0711.4646](#)].
- [11] L.J. Hall, K. Jedamzik, J. March-Russell and S.M. West, *Freeze-In Production of FIMP Dark Matter*, *JHEP* **03** (2010) 080 [[0911.1120](#)].
- [12] F. Elahi, C. Kolda and J. Unwin, *UltraViolet Freeze-in*, *JHEP* **03** (2015) 048 [[1410.6157](#)].
- [13] N. Bernal, M. Heikinheimo, T. Tenkanen, K. Tuominen and V. Vaskonen, *The Dawn of FIMP Dark Matter: A Review of Models and Constraints*, *Int. J. Mod. Phys. A* **32** (2017) 1730023 [[1706.07442](#)].
- [14] R. Allahverdi et al., *The First Three Seconds: a Review of Possible Expansion Histories of the Early Universe*, *Open J.Astrophys.* **04** (2021) [[2006.16182](#)].
- [15] P. Arias, N. Bernal, A. Herrera and C. Maldonado, *Reconstructing Non-standard Cosmologies with Dark Matter*, *JCAP* **10** (2019) 047 [[1906.04183](#)].
- [16] G. Kane, K. Sinha and S. Watson, *Cosmological Moduli and the Post-Inflationary Universe: A Critical Review*, *Int. J. Mod. Phys. D* **24** (2015) 1530022 [[1502.07746](#)].
- [17] R.T. Co, F. D’Eramo, L.J. Hall and D. Pappadopulo, *Freeze-In Dark Matter with Displaced Signatures at Colliders*, *JCAP* **12** (2015) 024 [[1506.07532](#)].
- [18] H. Davoudiasl, D. Hooper and S.D. McDermott, *Inflatable Dark Matter*, *Phys. Rev. Lett.* **116** (2016) 031303 [[1507.08660](#)].
- [19] L. Randall, J. Scholtz and J. Unwin, *Flooded Dark Matter and S Level Rise*, *JHEP* **03** (2016) 011 [[1509.08477](#)].
- [20] A. Berlin, D. Hooper and G. Krnjaic, *PeV-Scale Dark Matter as a Thermal Relic of a Decoupled Sector*, *Phys. Lett. B* **760** (2016) 106 [[1602.08490](#)].
- [21] T. Tenkanen and V. Vaskonen, *Reheating the Standard Model from a hidden sector*, *Phys. Rev. D* **94** (2016) 083516 [[1606.00192](#)].
- [22] J.A. Dror, E. Kuflik and W.H. Ng, *Codecaying Dark Matter*, *Phys. Rev. Lett.* **117** (2016) 211801 [[1607.03110](#)].
- [23] A. Berlin, D. Hooper and G. Krnjaic, *Thermal Dark Matter From A Highly Decoupled Sector*, *Phys. Rev. D* **94** (2016) 095019 [[1609.02555](#)].
- [24] F. D’Eramo, N. Fernandez and S. Profumo, *When the Universe Expands Too Fast: Relentless Dark Matter*, *JCAP* **05** (2017) 012 [[1703.04793](#)].
- [25] S. Hamdan and J. Unwin, *Dark Matter Freeze-out During Matter Domination*, *Mod. Phys. Lett. A* **33** (2018) 1850181 [[1710.03758](#)].
- [26] L. Visinelli, *(Non-)thermal production of WIMPs during kination*, *Symmetry* **10** (2018) 546 [[1710.11006](#)].
- [27] J.A. Dror, E. Kuflik, B. Melcher and S. Watson, *Concentrated dark matter: Enhanced small-scale structure from codecaying dark matter*, *Phys. Rev. D* **97** (2018) 063524 [[1711.04773](#)].

- [28] M. Drees and F. Hajkarim, *Dark Matter Production in an Early Matter Dominated Era*, *JCAP* **02** (2018) 057 [[1711.05007](#)].
- [29] F. D’Eramo, N. Fernandez and S. Profumo, *Dark Matter Freeze-in Production in Fast-Expanding Universes*, *JCAP* **02** (2018) 046 [[1712.07453](#)].
- [30] D. Maity and P. Saha, *Connecting CMB anisotropy and cold dark matter phenomenology via reheating*, *Phys. Rev. D* **98** (2018) 103525 [[1801.03059](#)].
- [31] N. Bernal, C. Cosme and T. Tenkanen, *Phenomenology of Self-Interacting Dark Matter in a Matter-Dominated Universe*, *Eur. Phys. J. C* **79** (2019) 99 [[1803.08064](#)].
- [32] E. Hardy, *Higgs portal dark matter in non-standard cosmological histories*, *JHEP* **06** (2018) 043 [[1804.06783](#)].
- [33] D. Maity and P. Saha, *CMB constraints on dark matter phenomenology via reheating in Minimal plateau inflation*, *Phys. Dark Univ.* **25** (2019) 100317 [[1804.10115](#)].
- [34] T. Hambye, A. Strumia and D. Teresi, *Super-cool Dark Matter*, *JHEP* **08** (2018) 188 [[1805.01473](#)].
- [35] N. Bernal, C. Cosme, T. Tenkanen and V. Vaskonen, *Scalar singlet dark matter in non-standard cosmologies*, *Eur. Phys. J. C* **79** (2019) 30 [[1806.11122](#)].
- [36] A. Arbey, J. Ellis, F. Mahmoudi and G. Robbins, *Dark Matter Casts Light on the Early Universe*, *JHEP* **10** (2018) 132 [[1807.00554](#)].
- [37] M. Drees and F. Hajkarim, *Neutralino Dark Matter in Scenarios with Early Matter Domination*, *JHEP* **12** (2018) 042 [[1808.05706](#)].
- [38] A. Betancur and Ó. Zapata, *Phenomenology of doublet-triplet fermionic dark matter in nonstandard cosmology and multicomponent dark sectors*, *Phys. Rev. D* **98** (2018) 095003 [[1809.04990](#)].
- [39] C. Maldonado and J. Unwin, *Establishing the Dark Matter Relic Density in an Era of Particle Decays*, *JCAP* **06** (2019) 037 [[1902.10746](#)].
- [40] A. Poulin, *Dark matter freeze-out in modified cosmological scenarios*, *Phys. Rev. D* **100** (2019) 043022 [[1905.03126](#)].
- [41] T. Tenkanen, *Standard model Higgs field and hidden sector cosmology*, *Phys. Rev. D* **100** (2019) 083515 [[1905.11737](#)].
- [42] C. Han, *Higgsino Dark Matter in a Non-Standard History of the Universe*, *Phys. Lett. B* **798** (2019) 134997 [[1907.09235](#)].
- [43] N. Bernal, F. Elahi, C. Maldonado and J. Unwin, *Ultraviolet Freeze-in and Non-Standard Cosmologies*, *JCAP* **11** (2019) 026 [[1909.07992](#)].
- [44] P. Chanda, S. Hamdan and J. Unwin, *Reviving Z and Higgs Mediated Dark Matter Models in Matter Dominated Freeze-out*, *JCAP* **01** (2020) 034 [[1911.02616](#)].
- [45] D. Mahanta and D. Borah, *TeV Scale Leptogenesis with Dark Matter in Non-standard Cosmology*, *JCAP* **04** (2020) 032 [[1912.09726](#)].
- [46] G. Arcadi, S. Profumo, F.S. Queiroz and C. Siqueira, *Right-handed Neutrino Dark Matter, Neutrino Masses, and non-Standard Cosmology in a 2HDM*, *JCAP* **12** (2020) 030 [[2007.07920](#)].
- [47] P. Konar, A. Mukherjee, A.K. Saha and S. Show, *A dark clue to seesaw and leptogenesis in a pseudo-Dirac singlet doublet scenario with (non)standard cosmology*, *JHEP* **03** (2021) 044 [[2007.15608](#)].
- [48] D. Bhatia and S. Mukhopadhyay, *Unitarity limits on thermal dark matter in (non-)standard cosmologies*, *JHEP* **03** (2021) 133 [[2010.09762](#)].

- [49] P. Arias, D. Karamitros and L. Roszkowski, *Frozen-in fermionic singlet dark matter in non-standard cosmology with a decaying fluid*, *JCAP* **05** (2021) 041 [[2012.07202](#)].
- [50] B. Barman, P. Ghosh, F.S. Queiroz and A.K. Saha, *Scalar multiplet dark matter in a fast expanding Universe: Resurrection of the desert region*, *Phys. Rev. D* **104** (2021) 015040 [[2101.10175](#)].
- [51] G. Arcadi, J.P. Neto, F.S. Queiroz and C. Siqueira, *Roads for right-handed neutrino dark matter: Fast expansion, standard freeze-out, and early matter domination*, *Phys. Rev. D* **105** (2022) 035016 [[2108.11398](#)].
- [52] D. Mahanta and D. Borah, *WIMPy Leptogenesis in Non-Standard Cosmologies*, [2208.11295](#).
- [53] J.D. Barrow, *Massive Particles as a Probe of the Early Universe*, *Nucl. Phys. B* **208** (1982) 501.
- [54] M. Kamionkowski and M.S. Turner, *Thermal Relics: Do we Know their Abundances?*, *Phys. Rev. D* **42** (1990) 3310.
- [55] J. McDonald, *WIMP Densities in Decaying Particle Dominated Cosmology*, *Phys. Rev. D* **43** (1991) 1063.
- [56] P. Salati, *Quintessence and the relic density of neutralinos*, *Phys. Lett. B* **571** (2003) 121 [[astro-ph/0207396](#)].
- [57] D. Comelli, M. Pietroni and A. Riotto, *Dark energy and dark matter*, *Phys. Lett. B* **571** (2003) 115 [[hep-ph/0302080](#)].
- [58] F. Rosati, *Quintessential enhancement of dark matter abundance*, *Phys. Lett. B* **570** (2003) 5 [[hep-ph/0302159](#)].
- [59] C. Pallis, *Massive particle decay and cold dark matter abundance*, *Astropart. Phys.* **21** (2004) 689 [[hep-ph/0402033](#)].
- [60] G.B. Gelmini and P. Gondolo, *Neutralino with the right cold dark matter abundance in (almost) any supersymmetric model*, *Phys. Rev. D* **74** (2006) 023510 [[hep-ph/0602230](#)].
- [61] G. Gelmini, P. Gondolo, A. Soldatenko and C.E. Yaguna, *The Effect of a late decaying scalar on the neutralino relic density*, *Phys. Rev. D* **74** (2006) 083514 [[hep-ph/0605016](#)].
- [62] A. Arbey and F. Mahmoudi, *SUSY constraints from relic density: High sensitivity to pre-BBN expansion rate*, *Phys. Lett. B* **669** (2008) 46 [[0803.0741](#)].
- [63] T. Cohen, D.E. Morrissey and A. Pierce, *Changes in Dark Matter Properties After Freeze-Out*, *Phys. Rev. D* **78** (2008) 111701 [[0808.3994](#)].
- [64] A. Arbey and F. Mahmoudi, *SUSY Constraints, Relic Density, and Very Early Universe*, *JHEP* **05** (2010) 051 [[0906.0368](#)].
- [65] G.F. Giudice, E.W. Kolb and A. Riotto, *Largest temperature of the radiation era and its cosmological implications*, *Phys. Rev. D* **64** (2001) 023508 [[hep-ph/0005123](#)].
- [66] N. Fornengo, A. Riotto and S. Scopel, *Supersymmetric dark matter and the reheating temperature of the universe*, *Phys. Rev. D* **67** (2003) 023514 [[hep-ph/0208072](#)].
- [67] M. Drees, H. Imminiyaz and M. Kakizaki, *Abundance of cosmological relics in low-temperature scenarios*, *Phys. Rev. D* **73** (2006) 123502 [[hep-ph/0603165](#)].
- [68] L. Roszkowski, S. Trojanowski and K. Turzyński, *Neutralino and gravitino dark matter with low reheating temperature*, *JHEP* **11** (2014) 146 [[1406.0012](#)].
- [69] S. Davidson, M. Losada and A. Riotto, *A New perspective on baryogenesis*, *Phys. Rev. Lett.* **84** (2000) 4284 [[hep-ph/0001301](#)].
- [70] R. Allahverdi, B. Dutta and K. Sinha, *Baryogenesis and Late-Decaying Moduli*, *Phys. Rev. D* **82** (2010) 035004 [[1005.2804](#)].

- [71] A. Beniwal, M. Lewicki, J.D. Wells, M. White and A.G. Williams, *Gravitational wave, collider and dark matter signals from a scalar singlet electroweak baryogenesis*, *JHEP* **08** (2017) 108 [[1702.06124](#)].
- [72] R. Allahverdi, P.S.B. Dev and B. Dutta, *A simple testable model of baryon number violation: Baryogenesis, dark matter, neutron–antineutron oscillation and collider signals*, *Phys. Lett. B* **779** (2018) 262 [[1712.02713](#)].
- [73] N. Bernal and C.S. Fong, *Hot Leptogenesis from Thermal Dark Matter*, *JCAP* **10** (2017) 042 [[1707.02988](#)].
- [74] S.-L. Chen, A. Dutta Banik and Z.-K. Liu, *Leptogenesis in fast expanding Universe*, *JCAP* **03** (2020) 009 [[1912.07185](#)].
- [75] M. Chakraborty and S. Roy, *Baryon asymmetry and lower bound on right handed neutrino mass in fast expanding Universe: an analytical approach*, [2208.04046](#).
- [76] H. Assadullahi and D. Wands, *Gravitational waves from an early matter era*, *Phys. Rev. D* **79** (2009) 083511 [[0901.0989](#)].
- [77] R. Durrer and J. Hasenkamp, *Testing Superstring Theories with Gravitational Waves*, *Phys. Rev. D* **84** (2011) 064027 [[1105.5283](#)].
- [78] L. Alabidi, K. Kohri, M. Sasaki and Y. Sendouda, *Observable induced gravitational waves from an early matter phase*, *JCAP* **05** (2013) 033 [[1303.4519](#)].
- [79] F. D’Eramo and K. Schmitz, *Imprint of a scalar era on the primordial spectrum of gravitational waves*, *Phys. Rev. Research*. **1** (2019) 013010 [[1904.07870](#)].
- [80] N. Bernal and F. Hajkarim, *Primordial Gravitational Waves in Nonstandard Cosmologies*, *Phys. Rev. D* **100** (2019) 063502 [[1905.10410](#)].
- [81] D.G. Figueroa and E.H. Tanin, *Ability of LIGO and LISA to probe the equation of state of the early Universe*, *JCAP* **08** (2019) 011 [[1905.11960](#)].
- [82] N. Bernal, A. Ghoshal, F. Hajkarim and G. Lambiase, *Primordial Gravitational Wave Signals in Modified Cosmologies*, *JCAP* **11** (2020) 051 [[2008.04959](#)].
- [83] M.A.G. Garcia, M. Pierre and S. Verner, *Scalar Dark Matter Production from Preheating and Structure Formation Constraints*, [2206.08940](#).
- [84] K. Kaneta, S.M. Lee and K.-y. Oda, *Boltzmann or Bogoliubov? Approaches compared in gravitational particle production*, *JCAP* **09** (2022) 018 [[2206.10929](#)].
- [85] R. Kallosh and A. Linde, *Universality Class in Conformal Inflation*, *JCAP* **07** (2013) 002 [[1306.5220](#)].
- [86] R. Kallosh, A. Linde and D. Roest, *Superconformal Inflationary α -Attractors*, *JHEP* **11** (2013) 198 [[1311.0472](#)].
- [87] A.A. Starobinsky, *A New Type of Isotropic Cosmological Models Without Singularity*, *Phys. Lett.* **91B** (1980) 99.
- [88] A.A. Starobinsky, *Nonsingular Model of the Universe with the Quantum Gravitational de Sitter Stage and its Observational Consequences*, in *Second Seminar on Quantum Gravity*, pp. 103–128, 1, 1981.
- [89] A.A. Starobinsky, *The Perturbation Spectrum Evolving from a Nonsingular Initially De-Sitter Cosmology and the Microwave Background Anisotropy*, *Sov. Astron. Lett.* **9** (1983) 302.
- [90] L. Kofman, A.D. Linde and A.A. Starobinsky, *Inflationary Universe Generated by the Combined Action of a Scalar Field and Gravitational Vacuum Polarization*, *Phys. Lett. B* **157** (1985) 361.

- [91] M.S. Turner, *Coherent Scalar Field Oscillations in an Expanding Universe*, *Phys. Rev. D* **28** (1983) 1243.
- [92] M.A.G. Garcia, K. Kaneta, Y. Mambrini and K.A. Olive, *Reheating and Post-inflationary Production of Dark Matter*, *Phys. Rev. D* **101** (2020) 123507 [2004.08404].
- [93] M.A.G. Garcia, K. Kaneta, Y. Mambrini and K.A. Olive, *Inflaton Oscillations and Post-Inflationary Reheating*, *JCAP* **04** (2021) 012 [2012.10756].
- [94] R.T. Co, E. Gonzalez and K. Harigaya, *Increasing Temperature toward the Completion of Reheating*, *JCAP* **11** (2020) 038 [2007.04328].
- [95] A. Ahmed, B. Grzadkowski and A. Socha, *Implications of time-dependent inflaton decay on reheating and dark matter production*, *Phys. Lett. B* **831** (2022) 137201 [2111.06065].
- [96] B. Barman, N. Bernal, Y. Xu and Ó. Zapata, *Ultraviolet freeze-in with a time-dependent inflaton decay*, *JCAP* **07** (2022) 019 [2202.12906].
- [97] A. Ahmed, B. Grzadkowski and A. Socha, *Higgs boson induced reheating and ultraviolet frozen-in dark matter*, 2207.11218.
- [98] P. Arias, N. Bernal, J.K. Osiński and L. Roszkowski, *Dark Matter Axions in the Early Universe with a Period of Increasing Temperature*, 2207.07677.
- [99] S. Sarkar, *Big bang nucleosynthesis and physics beyond the standard model*, *Rept. Prog. Phys.* **59** (1996) 1493 [hep-ph/9602260].
- [100] M. Kawasaki, K. Kohri and N. Sugiyama, *MeV scale reheating temperature and thermalization of neutrino background*, *Phys. Rev. D* **62** (2000) 023506 [astro-ph/0002127].
- [101] S. Hannestad, *What is the lowest possible reheating temperature?*, *Phys. Rev. D* **70** (2004) 043506 [astro-ph/0403291].
- [102] F. De Bernardis, L. Pagano and A. Melchiorri, *New constraints on the reheating temperature of the universe after WMAP-5*, *Astropart. Phys.* **30** (2008) 192.
- [103] P.F. de Salas, M. Lattanzi, G. Mangano, G. Miele, S. Pastor and O. Pisanti, *Bounds on very low reheating scenarios after Planck*, *Phys. Rev. D* **92** (2015) 123534 [1511.00672].
- [104] Y. Shtanov, J.H. Traschen and R.H. Brandenberger, *Universe reheating after inflation*, *Phys. Rev. D* **51** (1995) 5438 [hep-ph/9407247].
- [105] K. Ichikawa, T. Suyama, T. Takahashi and M. Yamaguchi, *Primordial Curvature Fluctuation and Its Non-Gaussianity in Models with Modulated Reheating*, *Phys. Rev. D* **78** (2008) 063545 [0807.3988].
- [106] K.D. Lozanov and M.A. Amin, *Equation of State and Duration to Radiation Domination after Inflation*, *Phys. Rev. Lett.* **119** (2017) 061301 [1608.01213].
- [107] D. Maity and P. Saha, *(P)reheating after minimal Plateau Inflation and constraints from CMB*, *JCAP* **07** (2019) 018 [1811.11173].
- [108] P. Saha, S. Anand and L. Sriramkumar, *Accounting for the time evolution of the equation of state parameter during reheating*, *Phys. Rev. D* **102** (2020) 103511 [2005.01874].
- [109] S. Antusch, D.G. Figueroa, K. Marschall and F. Torrenti, *Energy distribution and equation of state of the early Universe: matching the end of inflation and the onset of radiation domination*, *Phys. Lett. B* **811** (2020) 135888 [2005.07563].
- [110] R. Easther, R. Flauger and J.B. Gilmore, *Delayed Reheating and the Breakdown of Coherent Oscillations*, *JCAP* **04** (2011) 027 [1003.3011].
- [111] K. Freese, E.I. Sfakianakis, P. Stengel and L. Visinelli, *The Higgs Boson can delay Reheating after Inflation*, *JCAP* **05** (2018) 067 [1712.03791].

- [112] K. Harigaya, M. Kawasaki, K. Mukaida and M. Yamada, *Dark Matter Production in Late Time Reheating*, *Phys. Rev. D* **89** (2014) 083532 [[1402.2846](#)].
- [113] K. Harigaya, K. Mukaida and M. Yamada, *Dark Matter Production during the Thermalization Era*, *JHEP* **07** (2019) 059 [[1901.11027](#)].
- [114] M. Drees and B. Najjari, *Energy spectrum of thermalizing high energy decay products in the early universe*, *JCAP* **10** (2021) 009 [[2105.01935](#)].
- [115] M. Drees and B. Najjari, *Multi-Species Thermalization Cascade of Energetic Particles in the Early Universe*, [2205.07741](#).
- [116] K. Mukaida and M. Yamada, *Cascades of high-energy SM particles in the primordial thermal plasma*, [2208.11708](#).
- [117] PARTICLE DATA GROUP collaboration, *Review of Particle Physics*, *PTEP* **2020** (2020) [083C01](#).
- [118] R.K. Leane, T.R. Slatyer, J.F. Beacom and K.C.Y. Ng, *GeV-scale thermal WIMPs: Not even slightly ruled out*, *Phys. Rev. D* **98** (2018) 023016 [[1805.10305](#)].
- [119] HESS, HAWC, VERITAS, MAGIC, H.E.S.S., FERMI-LAT collaboration, *Combined dark matter searches towards dwarf spheroidal galaxies with Fermi-LAT, HAWC, H.E.S.S., MAGIC, and VERITAS*, *PoS ICRC2021* (2021) 528 [[2108.13646](#)].
- [120] L. Bergstrom, T. Bringmann, I. Cholis, D. Hooper and C. Weniger, *New Limits on Dark Matter Annihilation from AMS Cosmic Ray Positron Data*, *Phys. Rev. Lett.* **111** (2013) [171101](#) [[1306.3983](#)].
- [121] F. Calore, M. Cirelli, L. Derome, Y. Genolini, D. Maurin, P. Salati et al., *AMS-02 antiprotons and dark matter: Trimmed hints and robust bounds*, *SciPost Phys.* **12** (2022) 163 [[2202.03076](#)].
- [122] M. Zemp, J. Diemand, M. Kuhlen, P. Madau, B. Moore, D. Potter et al., *The Graininess of Dark Matter Haloes*, *Mon. Not. Roy. Astron. Soc.* **394** (2009) 641 [[0812.2033](#)].
- [123] M. Pato, O. Agertz, G. Bertone, B. Moore and R. Teyssier, *Systematic uncertainties in the determination of the local dark matter density*, *Phys. Rev. D* **82** (2010) 023531 [[1006.1322](#)].
- [124] N. Bernal, J.E. Forero-Romero, R. Garani and S. Palomares-Ruiz, *Systematic uncertainties from halo asphericity in dark matter searches*, *JCAP* **09** (2014) 004 [[1405.6240](#)].
- [125] M. Boudaud et al., *A new look at the cosmic ray positron fraction*, *Astron. Astrophys.* **575** (2015) A67 [[1410.3799](#)].
- [126] N. Bernal, J.E. Forero-Romero, R. Garani and S. Palomares-Ruiz, *Systematic uncertainties from halo asphericity in dark matter searches*, *Nucl. Part. Phys. Proc.* **267-269** (2015) 345.
- [127] N. Bernal, L. Necib and T.R. Slatyer, *Spherical Cows in Dark Matter Indirect Detection*, *JCAP* **12** (2016) 030 [[1606.00433](#)].
- [128] M. Benito, N. Bernal, N. Bozorgnia, F. Calore and F. Iocco, *Particle Dark Matter Constraints: the Effect of Galactic Uncertainties*, *JCAP* **02** (2017) 007 [[1612.02010](#)].
- [129] CTA collaboration, *Sensitivity of the Cherenkov Telescope Array to a dark matter signal from the Galactic centre*, *JCAP* **01** (2021) 057 [[2007.16129](#)].